Volume 51 | Number 87 | 11 November 2015 | Pages 15741–15868

ChemComm

Chemical Communications

www.rsc.org/chemcomm

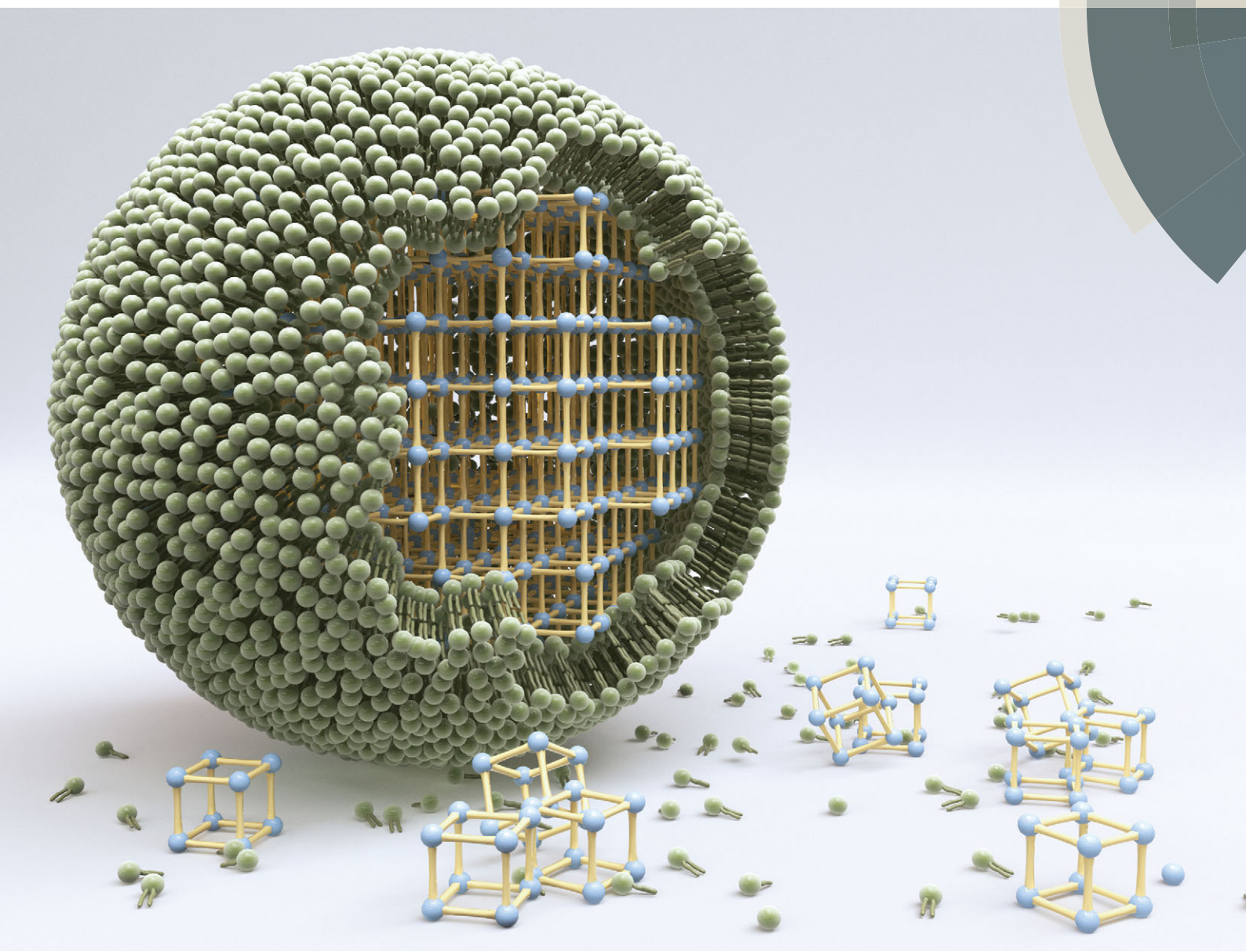

ISSN 1359-7345

ROYAL SOCIETY OF CHEMISTRY

COMMUNICATION

Stefan Wuttke, Thomas Bein *et al.*

MOF nanoparticles coated by lipid bilayers and their uptake by cancer cells

ChemComm

COMMUNICATION

View Article Online
View Journal | View Issue

Cite this: *Chem. Commun.*, 2015, **51**, 15752

Received 12th August 2015,
Accepted 4th September 2015

DOI: 10.1039/c5cc06767g

www.rsc.org/chemcomm

MOF nanoparticles coated by lipid bilayers and their uptake by cancer cells†

Stefan Wuttke,*[a] Simone Braig,‡[b] Tobias Preiß,‡[c] Andreas Zimpel,[a] Johannes Sicklinger,[a] Claudia Bellomo,[a] Joachim O. Rädler,[c] Angelika M. Vollmar[b] and Thomas Bein*[a]

We report the synthesis of MOF@lipid nanoparticles as a versatile and powerful novel class of nanocarriers based on metal–organic frameworks (MOFs). We show that the MOF@lipid system can effectively store dye molecules inside the porous scaffold of the MOF while the lipid bilayer prevents their premature release. Efficient uptake of the MOF@lipid nanoparticles by cancer cells makes these nanocarriers promising for drug delivery and diagnostic purposes.

The chemical synthesis of well-defined functional nano-objects is one of the intriguing challenges of nanoscience. In this context metal–organic frameworks (MOFs) offer the ability to generate crystallographically defined, functionalized, porous nanocrystals. MOFs consist of inorganic clusters acting as nodes connected by organic linker molecules. Together, these building blocks create three-dimensional porous crystalline networks with very high pore volume and surface area. The large range of possible compositions (metals, linkers), the structural diversity (pore size, structure, *etc.*) and the numerous options to functionalize these porous crystalline hybrid inorganic–organic solids make them attractive for different fields of applications such as small molecule storage (H_2, CH_4, CO_2, *etc.*), catalysis, separation, luminescence, magnetism and other applications.[1–4] In addition, MOFs can be scaled down to nanometer size, which makes them potentially useful as nanocarriers in medical applications.[5]

Incorporating drug molecules into nanocarriers offers exciting opportunities to redefine the pharmacokinetic behavior of the drug, improving its therapeutic efficiency and reducing side effects.[6–8] Several types of drug delivery nanocarriers based on organic platforms such as liposomes, polymers, and dendrimers have been used as "smart" systems that can release therapeutic agents under physicological conditions. Recent research has also addressed the potential of inorganic nanoparticles such as gold, iron oxide or mesoporous silica in this context.[9] The high loading capacity of MOFs for bioactive molecules and their applications for drug delivery and imaging purposes have recently been demonstrated.[5] However, the controlled retention of cargo inside the MOF nanoparticles (NPs) and its controlled release is a challenge that still needs to be addressed.[5,10–15]

Here we report on the synthesis of MOF nanoparticle-supported lipid bilayers – MOF@lipid – that synergistically combine properties of liposomes and porous particles. Our aim was to develop a novel route for the flexible, non-covalent encapsulation of biologically active molecules into porous MOF networks that can ultimately serve as functional MOF@lipid nanocarriers for controlled drug delivery or imaging purposes. Conceptually, a MOF@lipid nanoparticle may offer three key advantages in comparison to a liposome. First, surface modifications (*e.g.* modifying the size or the hydrophilic/hydrophobic nature of the pores) of the MOF nanoparticle can control the uptake and release kinetics of the drug.[5,16] In addition, a MOF@lipid nanoparticle is expected to be significantly more stable than a liposome, which has an aqueous core instead of a porous MOF core. Finally, due to their high porosity MOF nanoparticles have been shown to offer exceptionally high loading capacities compared to other nanocarrier systems.[5,11]

To demonstrate our new strategy, we chose the mesoporous iron(III) carboxylate MIL-100(Fe)[17] and the mesoporous chromium(III) carboxylate MIL-101(Cr).[18] MIL-100(Fe) is built up from octahedral trimers connected by trimesate (benzene-1,3,5-tricarboxylate) resulting in a MOF scaffold with large pores (diameter 2.4–2.9 nm) and window sizes (0.6–0.9 nm). MIL-101(Cr) is built up from octahedral trimers connected by terephthalate (benzene-1,4-dicarboxylate), also resulting in a MOF scaffold with large pores (diameter 2.9–3.4 nm) and window sizes (1.2–1.7 nm). Moreover, nanoparticle synthesis is already established for both structures.[11,19]

Both MOF nanoparticles (NPs) were synthesized in a microwave oven from Anton Paar (Synthos 3000). MIL-100(Fe) NPs were obtained by reacting $FeCl_3 \cdot 6H_2O$ and trimesic acid in a

[a] *Department of Chemistry and Center for NanoScience (CeNS), University of Munich (LMU), Butenandtstraße 11 (E), 81377 München, Germany. E-mail: stefan.wuttke@cup.uni-muenchen.de, bein@cup.lmu.de*
[b] *Department of Pharmacy University of Munich (LMU), Butenandtstraße 5, 81377 München, Germany*
[c] *Faculty of Physics and Center for NanoScience (CeNS), University of Munich (LMU), Geschwister Scholl Platz 1, 80539 München, Germany*
† Electronic supplementary information (ESI) available. See DOI: 10.1039/c5cc06767g
‡ These authors contributed equally.

9 : 4 molar ratio in H_2O, using a temperature controlled microwave program (heating to 130 °C in 30 s and holding at that temperature for 2 min). MIL-101(Cr) nanoparticles were synthesized from an equimolar mixture of terephthalic acid and $Cr(NO_3)_3 \cdot 9H_2O$ in H_2O, using a temperature controlled microwave program (heating to 180 °C in 4 min and holding at that temperature for 2 min). The resulting nanoparticles show the characteristic XRD reflections of the MOFs, with line broadening due to the small particle size (Fig. S6 and S7, ESI†).[18,19] The estimated size distribution of MIL-100(Fe) obtained transmission electron microscopy (TEM) is in the range of 54 ± 24 nm (Fig. S11, ESI†). For MIL-101(Cr), it is in the range of 49 ± 20 nm (Fig. S10, ESI†). In addition, TEM images (Fig. S12 and S13, ESI†) confirm the high crystalline quality of the nanocrystals. The calculation of the BET specific surface area based on nitrogen sorption isotherms gave a value of 2004 $m^2\ g^{-1}$ for nanoscale MIL-100(Fe) (Fig. S14, ESI†) and 3205 $m^2\ g^{-1}$ for nanoscale MIL-101(Cr) (Fig. S15, ESI†), which is similar to reported data.[18,19]

In the next step, MIL-100(Fe) and MIL-101(Cr) nanoparticles were coated with a lipid bilayer using the lipid DOPC (1,2-dioleoyl-*sn*-*glycero*-3-phosphocholine). The principle of the coating procedure is a controlled solvent-exchange deposition of the lipid onto the MOF surface.[20] For this purpose the lipid and the MOF nanoparticles are dispersed in an EtOH/H_2O mixture, where the lipids exist as monomers.[21] When the water concentration is drastically increased, the lipids precipitate on the nanoparticle surface and form a lipid bilayer (Fig. 1). The successful coating of the MOF nanoparticles with lipid was confirmed by different techniques.

The diffraction pattern of the two DOPC-coated nanoparticles shows the same reflections as the uncoated nanoparticles (Fig. S6 and S7, ESI†). Hence, the MOF structures were stable during the procedure of lipid layer coating. Dynamic light scattering (DLS) data of the MIL-101(Cr)@DOPC nanoparticles showed an increased diameter of 78 ± 22 nm (*vs.* 69 ± 19 nm for the pure MIL-101(Cr) nanoparticles, Fig. S16, ESI†). This shift of the hydrodynamic diameter of about 10 nm is close to the expected value.[19] Time series of DLS measurements of MIL-100(Fe) and MIL-100(Fe)@DOPC nanoparticles reveal the colloidal stability of the lipid-coated versions whereas the pure nanoparticles agglomerate in a matter of hours (Fig. S18 and S19, ESI†). Therefore, the supported lipid can serve not only as a cap system to store molecules inside the MOF nanoparticles but also to increase their colloidal stability, which is of great importance for biomedical applications.

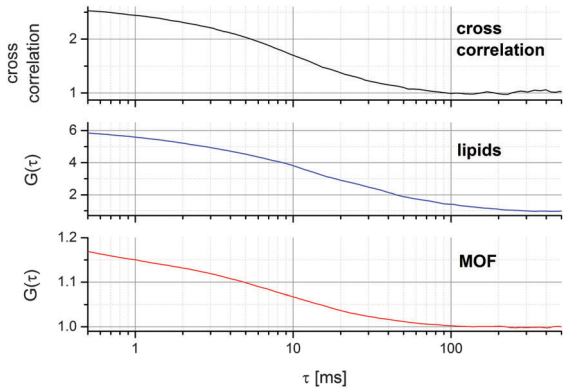

Fig. 2 FCCS of DOPC lipids (BODIPY labeled) on MIL-101(Cr) nanoparticles (Atto633 labeled). The high cross-correlation amplitude indicates the co-localization of lipids and MOF nanoparticles.

In order to confirm the localization of the lipids on the MOF nanoparticles in solution, both components were labelled and fluorescence cross-correlation analysis (FCCS) was performed. FCCS provides evidence for correlated movement of two differently labelled species within the confocal detection volume, by cross-correlating the fluorescence fluctuation signal of both species.[22,23] Fig. 2 shows the auto-correlation curves of the Atto633-labeled MIL-101(Cr) and BODIPY-FL-DHPE-labelled DOPC lipids as well as the cross-correlation. The analysis of the cross-correlation shows a high ratio of co-localization of lipids and MOF particles and hence proves the successful lipid coating of the MOF nanoparticle. For the MIL-100(Fe) we found that the fluorescence of different fluorescence dyes is completely quenched. Therefore, FCCS measurements for the MIL-100(Fe)@DOPC system are not applicable. However, we performed fluorescence correlation spectroscopy (FCS) measurements with BODIPY FL DHPE-labelled DOPC lipids alone and with unlabelled MIL-100(Fe) NPs (Fig. S2, ESI†). Juxtaposition of both sample results shows both a completely different count rate and correlation curve, respectively. This strongly indicates an interaction of MIL-100(Fe) NPs with lipids.

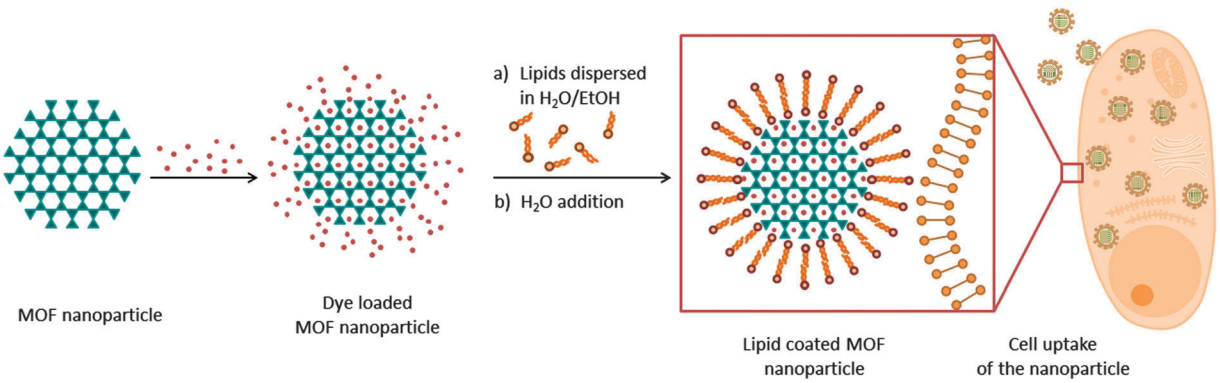

Fig. 1 Schematic description of the synthesis of lipid bilayer-coated MOF nanoparticles loaded with dye molecules and their uptake in cancer cells.

To confirm the successful lipid coating of the porous nanoparticles with another technique, and more importantly, to investigate the sealing properties of the lipid bilayer, we carried out fluorescence release experiments. For this purpose MIL-101(Cr) and MIL-100(Fe) nanoparticles were loaded with fluorescein dye and the dye was encapsulated in the nanoparticles through the formation of the lipid bilayer (Fig. 1). These dye-loaded nanoparticles were transferred into the cap of a fluorescence cuvette that was subsequently sealed with a dialysis membrane. Only free dye molecules, but not nanoparticles, can pass the membrane into the cuvette volume filled with water where the fluorescence measurement is recorded. Consequently, only dye molecules released from the pores of the particles contribute to the fluorescence intensity measured in the cuvette (detailed information is reported in the ESI†).

Fig. 3 shows the result of a typical fluorescence release experiment with MIL-101(Cr); the corresponding experiment with MIL-100(Fe) can be found in the ESI† (Fig. S20). The fluorescence intensity released from DOPC-coated MIL-101(Cr) nanoparticles reached only very low values after 1 h. Hence, we conclude that the dye is retained in the nanoparticles and that the dye molecules do not permeate through the DOPC bilayer. After one hour of monitoring without any significant increase of the fluorescence intensity, the nonionic surfactant triton X-100 was added into the cap. After a short induction period, the fluorescence intensity showed a rapid increase, which subsequently slowed over time. Release kinetics of the dye show a burst release within the first 30 min, which is relatively small in comparison with other nanocarriers,[9,21] and afterwards a release that is mainly governed by diffusion processes combined with dye–host interactions. Such behaviour can be advantageous for later applications as a drug carrier, because the drug release rate can be controlled by tuning the pore size and shape as well as the functionality of the MOF nanocarrier, and at the same time high burst release effects can be avoided, ensuring a fairly constant drug release. Therefore, the structural features of MOFs including crystalline porosity and widely tunable functionality are advantageous for controlling host–guest interactions.

The above results demonstrate the successful creation of a lipid bilayer around MOF nanoparticles that enables encapsulation of a dye or other molecules inside the MOF scaffold.

For future applications of MOF@lipid systems in biomedicine, the cellular uptake of these constructs is of particular interest. Due to the quenching effect of the MIL-100(Fe) nanoparticles, corresponding fluorescence tracking experiments can be only done with the MIL-101(Cr)@DOPC nanoparticles. For this purpose, 20 000 T24 bladder carcinoma cells per well with 250 μl medium were incubated with 20 μl of a suspension of Atto633 labelled MIL-101(Cr)@DOPC NPs (c = 1 mg ml^{-1}). Co-staining with PKH26, a red fluorescent dye that stains cellular membranes incorporating biolipid structures, revealed enrichment of MOF nanoparticles in cellular vesicles over time as demonstrated by confocal laser scanning microscopy. As shown in Fig. 4, strong accumulation of the MOF particles in cellular vesicles is detectable within 6 h and persists for at least 48 h. To investigate whether the MOF@lipid nanoparticles alter the cellular behaviour and/or condition, an impedance-based real time monitoring (xCELLigence System) approach was used. Importantly, xCELLigence analysis showed that both MOF@lipid nanoparticle systems themselves have no cytotoxic or anti-proliferative effect on the cancer cells (Fig. S21 and S22, ESI†).

In summary, we have developed novel metal–organic framework nanoparticles encapsulated by a lipid membrane. We have demonstrated that the MOF@lipid system can effectively store dye molecules inside the porous scaffold of the MOF while the lipid bilayer prevents their premature release. Moreover, for MIL-100(Fe) the lipid bilayer drastically increases the colloidal stability of the nanoparticles. Employing fluorescence microscopy, we were able to demonstrate the high uptake of lipid-coated nanoparticles by cancer cells. Considering the various ways to synthesize different functionalized MOF nanoparticles

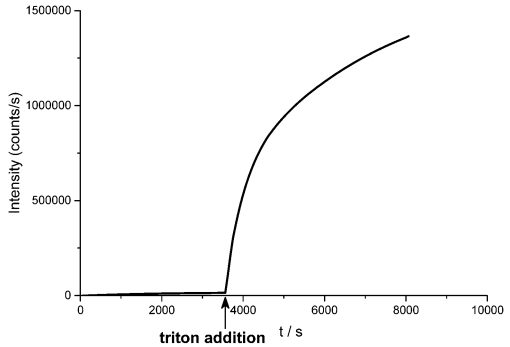

Fig. 3 Fluorescence release experiments of encapsulated fluorescein in MIL-101(Cr)@DOPC nanoparticles (the data points correspond to the intensities at the peak maxima at 512 nm for fluorescein). After 1 hour of measuring time with no significant increase of the fluorescence intensity, triton was added to the cap system. The destabilization of the lipid bilayer can be observed in the release of the fluorescein dye. The measurement took place at 37 °C and was stopped after 2 h of fluorescein dye release due to an oversaturation of the detector (intensity maximum of the detector 2 million counts per second).

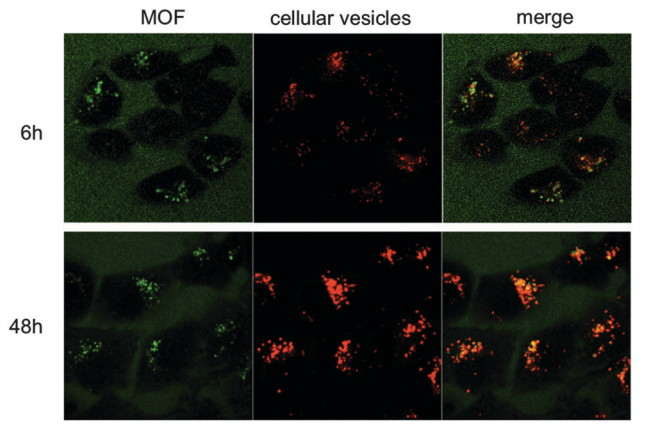

Fig. 4 Cellular uptake of MOF nanoparticles in cancer cells as monitored by confocal laser scanning microscopy. Bladder cancer cells were incubated with fluorescently-labelled MOF particles for 6 h and 48 h and co-stained with the membrane marker PKH26 to confirm enrichment of MOF in cellular vesicles.

as well as the richness of lipids with diverse functions (cap system, triggered release, incorporation of shielding ligand for long circulation times and targeting functions),[24,25] MOF@lipid nanoparticles have great potential as a novel hybrid nanocarrier system. On the one hand, the MOF core could store different active species such as imaging, diagnostic or drug molecules, and on the other hand the lipid shell could be used for the incorporation of targeting or shielding ligands (*e.g.* PEG) as well as for the creation of triggered release mechanisms. Based on the above results with lipid layers serving as model systems, we anticipate further progress in the synthesis of well-defined multifunctional MOF@lipid nanoparticles for drug delivery and diagnostic purposes and the clinical implementation of this nanotechnology.

The authors are grateful for financial support from the Deutsche Forschungsgemeinschaft (DFG) through the SFB 1032 and the DFG-project WU 622/4-1, the Excellence Cluster Nanosystems Initiative Munich (NIM) and the Center for Nano-Science Munich (CeNS).

Notes and references

1 Theme issue: Metal–Organic Frameworks, H.-C. Zhou, J. R. Long and O. M. Yaghi, *Chem. Rev.*, 2012, **112**, 673.
2 Theme issue: Metal–Organic Frameworks, H.-C. J. Zhou and S. Kitagawa, *Chem. Soc. Rev.*, 2014, **43**, 5415.
3 G. Férey, *Chem. Soc. Rev.*, 2008, **37**, 191.
4 H. Furukawa, K. E. Cordova, M. O'Keeffe and O. M. Yaghi, *Science*, 2013, **341**, 974.
5 P. Horcajada, R. Gref, T. Baati, P. K. Allan, G. Maurin, P. Couvreur, G. Férey, R. E. Morris and C. Serre, *Chem. Rev.*, 2012, **112**, 1232.
6 D. Peer, J. M. Karp, S. Hong, O. C. Farokhazad, R. Margalit and R. Langer, *Nat. Nanotechnol.*, 2007, **2**, 751.
7 M. E. Davis, Z. Chen and D. M. Shin, *Nat. Rev. Drug Discovery*, 2008, **7**, 771.
8 K. K. Cati, M. E. Belowich, M. Liong, M. W. Ambrogio, Y. A. Lau, H. A. Khativ, J. I. Zink, N. M. Khashab and J. F. Stoddart, *Nanoscale*, 2009, **1**, 16.
9 Z. Li, J. C. Barnes, A. Bosoy, J. F. Stoddart and J. I. Zink, *Chem. Soc. Rev.*, 2012, **41**, 2590.
10 V. Agostoni, P. Horcajada, M. Noiray, M. Malanga, A. Akykac, L. Jicsinszky, A. Vargas-Berenguel, N. Semiramoth, S. Daoud-Mahammed, V. Nicolas, C. Martineau, F. Taulelle, J. Vigneron, A. Etcheberry, C. Serre and R. Gref, *Sci. Rep.*, 2014, **5**, 7925.
11 P. Horcajada, T. Chalati, C. Serre, B. Gillet, C. Sebrie, T. Baati, J. F. Eubank, D. Heurtaux, P. Clayette, C. Kreuz, J.-S. Chang, Y. K. Hwang, V. Marsaud, P.-N. Bories, L. Cynober, S. Gil, G. Férey, P. Couvreur and R. Gref, *Nat. Mater.*, 2010, **9**, 172.
12 K. Khaletskaya, J. Reboul, M. Meilikhov, M. Nakahama, S. Diring, M. Tsujimoto, S. Isoda, F. Kim, K. Kamei, R. A. Fischer, S. Kitagawa and S. Furukawa, *J. Am. Chem. Soc.*, 2013, **135**, 10998.
13 S. Diring, D. O. Wang, C. Kim, M. Kondo, Y. Chen, S. Kitagawa, K. Kamei and S. Furukawa, *Nat. Commun.*, 2013, **4**, 2684.
14 C. He, K. Lu, D. Liu and W. Lin, *J. Am. Chem. Soc.*, 2014, **136**, 5181.
15 A. C. McKinlay, P. K. Allan, C. L. Renouf, M. J. Duncan, P. S. Wheatley, S. J. Warrender, D. Dawson, S. E. Ashbrook, B. Gil, B. Marszalek, T. Düren, J. J. Williams, C. Charrier, D. K. Mercer, S. J. Teat and R. E. Morris, *APL Mater.*, 2014, **2**, 124108.
16 D. Cunha, M. B. Yahia, S. Hall, S. R. Miller, H. Chevreau, E. Elkaim, G. Maurin, P. Horcajada and C. Serre, *Chem. Mater.*, 2013, **25**, 2767.
17 P. Horcajada, S. Surblé, C. Serre, D.-Y. Hong, Y.-K. Seo, J.-S. Chang, J.-M. Grenèche, I. Margiolaki and G. Férey, *Chem. Commun.*, 2007, 2820.
18 G. Férey, C. Mellot-Draznieks, C. Serre, F. Millange, J. Dutour, S. Surblé and I. Margiolaki, *Science*, 2005, **309**, 2040.
19 A. Demessence, P. Horcajada, C. Serre, C. Boissière, D. Grosso, C. Sanchez and G. Férey, *Chem. Commun.*, 2009, 7149.
20 A. O. Hohner, M. P. David and J. O. Rädler, *Biointerphases*, 2010, **5**, 1.
21 V. Cauda, H. Engelke, A. Sauer, D. Arcizet, C. Bräuchle, J. Rädler and T. Bein, *Nano Lett.*, 2010, **107**, 2484.
22 R. Rigler, *J. Biotechnol.*, 1995, **41**, 177.
23 S. Maiti, U. Haupts and W. W. Webb, *Biophys. J.*, 1997, **72**, 1878.
24 T. M. Allen and P. R. Cullis, *Adv. Drug Delivery Rev.*, 2013, **65**, 36.
25 B. Kneidl, M. Peller, G. Winter, L. H. Lindner and M. Hossann, *Int. J. Nanomed.*, 2014, **4**, 4387.